JOURNAL OF VIROLOGY, Jan. 2005, p. 1036–1044 Vol. 79, No. 2
0022-538X/05/$08.00+0 doi:10.1128/JVI.79.2.1036–1044.2005

Natural History of a Recurrent Feline Coronavirus Infection and the Role of Cellular Immunity in Survival and Disease

Jolanda D. F. DE Groot-Mijnes,[1]† Jessica M. VAN Dun,[1] Robbert G. VAN DER Most,[2] and Raoul J. DE Groot[1]*

Virology Division[1] and Immunology Division,[2] Department of Infectious Diseases and Immunology, Faculty of Veterinary Medicine, Utrecht University, Utrecht, The Netherlands

Received 22 June 2004/Accepted 16 August 2004

We describe the natural history, viral dynamics, and immunobiology of feline infectious peritonitis (FIP), a highly lethal coronavirus infection. A severe recurrent infection developed, typified by viral persistence and acute lymphopenia, with waves of enhanced viral replication coinciding with fever, weight loss, and depletion of $CD4^+$ and $CD8^+$ T cells. Our combined observations suggest a model for FIP pathogenesis in which virus-induced T-cell depletion and the antiviral T-cell response are opposing forces and in which the efficacy of early T-cell responses critically determines the outcome of the infection. Rising amounts of viral RNA in the blood, consistently seen in animals with end-stage FIP, indicate that progression to fatal disease is the direct consequence of a loss of immune control, resulting in unchecked viral replication. The pathogenic phenomena described here likely bear relevance to other severe coronavirus infections, in particular severe acute respiratory syndrome, for which multiphasic disease progression and acute T-cell lymphopenia have also been reported. Experimental FIP presents a relevant, safe, and well-defined model to study coronavirus-mediated immunosuppression and should provide an attractive and convenient system for in vivo testing of anticoronaviral drugs.

The genus *Coronavirus* (family *Coronaviridae*, order *Nidovirales*) comprises a group of enveloped positive-strand RNA viruses of mammals and birds. With a genome of 27 to 31 kb, encoding an ~750-kDa pp1ab replicase polyprotein, four structural proteins (S, M, N, and E) and up to five accessory nonstructural proteins, coronaviruses (CoVs) are the largest RNA viruses known to date (5, 11). In humans, they are mostly associated with mild enteric or respiratory infections, such as the common cold, and hence were long considered of modest clinical importance. However, the sudden emergence of severe acute respiratory syndrome (SARS) has sparked wide interest in CoV biology and pathogenesis (12, 22, 23, 34, 36). The more recent discovery of yet another human CoV, HCoV-NL63 (14, 45), also implicated in severe respiratory disease, further emphasizes the pathogenic potential of CoVs and stresses the need for the development of new prophylactic and therapeutic strategies.

Among the most conspicuous clinicopathological findings reported for SARS are the protracted multiphasic course of the infection with recurrence of fever and disease after initial apparent improvement and a consistent $CD4^+$ and $CD8^+$ T-cell lymphopenia (4, 8, 23, 36, 44, 56). In this respect, there are striking similarities with a lethal CoV infection occurring in cats. Feline infectious peritonitis (FIP) is a progressive debilitating condition caused by FIP viruses (FIPVs) (for a review, see reference 9), pathogenic virulence mutants spontaneously arising from apathogenic feline enteric CoV field strains (18, 35, 49). Typical for the disease are the widespread pyogranulomatous lesions, which occur in various tissues and organs, including lung, liver, spleen, omentum, and brain (32, 50, 54). The infection of macrophages and monocytes is thought to be key to the pathogenic mechanism (40, 52). There is ample evidence for a crucial involvement of the immune system. A profound T-cell depletion from the periphery and the lymphatic tissues, observed in cats with end-stage FIP (16, 21), and the common occurrence of hypergammaglobulinemia (29, 50) are indicative of a severe virus-induced immune dysregulation (20). The humoral response against FIPV does not seem to be protective and can in fact lead to "early death syndrome," a more fulminating and drastically shortened course of the disease (31, 52). Antibodies directed against the spike protein S, when present at subneutralizing titers, apparently opsonize the virus and enhance the infection of target cells via Fc receptor-mediated attachment (7, 19, 47). It is commonly believed that the control of infection and FIPV clearance are primarily achieved through cell-mediated immunity (CMI) (17, 35, 51).

Here, we present a comprehensive study of the natural history and immunobiology of FIP, based upon longitudinal infection experiments performed with the highly virulent FIPV strain 79–1146. We show that FIPV causes a multiphasic recurrent infection with waves of enhanced FIPV replication coinciding with fever, weight loss, and a dramatic decline in peripheral $CD4^+$ and $CD8^+$ T-cell counts. Consistent with the notion that CMI is protective, we detected FIPV-specific Th1 T-cell responses in surviving animals with the spike protein S as the main $CD8^+$ T-cell antigen. A model is discussed in which cellular immunity is counteracted by virus-induced T-cell depletion and in which the efficacy of the initial T-cell responses

* Corresponding author. Mailing address: Virology Division, Department of Infectious Diseases and Immunology, Faculty of Veterinary Medicine, Utrecht University, Yalelaan 1, 3584 CL Utrecht, The Netherlands. Phone: 31 30 2531463. Fax: 31 30 2536723. E-mail: R.Groot@vet.uu.nl.

† Present address: Department of Virology, Eijkman-Winkler Center, University Medical Center Utrecht, Utrecht, The Netherlands.

TABLE 1. Clinicopathological manifestations in FIPV-infected cats

Cat no.	Disease type	Vaccination history[a]	DPI[b]	Clinical signs[c]	Viremia	FIP	Exudate[d]	Lesions[e]
307	A	C	18	WL, F, L, J	+	+	Th	Lu, P
315	A	M1	21	WL, F, L, J	+	+	Pe	Li, K, S, I
007	A	A	21	WL, F, L, J	+	+	Pe, Th	Lu, (Li), I
081	A	A	21	WL, F, L, J	+	+	Pe, Th	Lu, K, (S), I
089	A	A	21	WL, F, L, J	+	+	Pe	Li, S, I
319	A	C	22	WL, F, L, J	+	+	Th, (Pe)	Lu, (P), Li, (K), S
283	A	C	24	WL, F, L, J	+	+		Lu, Li, K, S
299	A	C	24	WL, F, L, J	+	+	Pe	Lu, Li, I
157	A	M2	16	WL, F, L, J	+	+	Th	Lu, (S)
199	A	M2	16	WL, F, L, J	+	+	Pe	Li, S, I
145	A	A–D	22	WL, F, L, J	+	+	Pe, (Th)	Lu, Li, (K), S, I
147	A	M2	25	WL, F, L, J	+	+	Pe, Th	Lu, P, Li, S, I
201	A	A–D	22	WL, F, L, J	+	+	Pe, (Th)	Lu, Li, S
325	B	C	27	WL, F, L, J	+	+	Pe, Th	Lu, P, Li, S, I
301	B	C	28	WL, F, L, J	+	+	Pe	Lu, Li, K, (S), I
083	B	C	28	WL, F, L, J	+	+	Pe, Th	Lu, (Li, S), I
149	B	A–D	29	WL, F, L, J	+	+	Pe	Li, S, I
159	B	A–D	29	WL, F, L, J	+	+	Pe	(Li,) S, I
173	B	M2	28	WL, F, L, J	+	+	Pe, Th	Lu, Li, S, I
303	C	M1	36	WL, F, L, J	+	+	Pe, Th	Lu, P, Li, S, I
041	C	M1	35	WL, F, L, J	+	+	Th	Lu, P, Li, K, (S), I
009	C	A	35	WL, F, L, J	+	+	Pe	Lu, P, (Li, S), I
197	C	M2	34	WL, F, L, J	+	+		Lu, (P), Li, S, I
317	D	A	54	WL, F, L, J	+	+	Pe	Lu, P, Li, S, I
175	D	A–D	50	WL, F, L, J	+	+	Pe	Li, S
085	NA[f]	M1	58	WL, F, L, J	+	−		
155	NA[f]	M2	42	WL, F, L, J	+	−		
281	E	M1	>100	WL, F, L, J	+	−		
289	E	M1	>100	WL, F, L, J	+	−		
005	E	M1	>100	WL, F, L, J	+	−		
291	E	A	>100	WL, F, L, J	−	−		
297	E	A	>100	WL, F, L, J	+	−		
249[g]	E	NA[f]	>100	WL, F, L, J	ND[f]	−		

[a] M1, mock vaccinated with two doses of 0.5 mg of a pcDNA vector carrying the *lacZ* gene intradermally (i.d.) and one dose of 1×10^8 PFU of rVV-TK$^-$ i.d. at 6-week intervals; M2, mock vaccinated with one dose of 0.125 mg of a pcDNA vector carrying the *lacZ* gene both i.d. and intramuscularly (i.m.) and one dose of 1×10^8 rVV-TK$^-$ i.d. at 6-week intervals; A, POLA vaccinated with two doses of 0.5 mg of a pcDNA vector expressing POLA i.d. and one dose of 1×10^8 PFU of rVV-POLA i.d. at 6-week intervals; C, POLC vaccinated with two doses of 0.5 mg of a pcDNA vector expressing POLC i.d. and 1 dose of 1×10^8 PFU of rVV-POLC i.d. at 6-week intervals; A–D, POLA-D vaccinated with one dose of a mixture of 0.125 mg (each) of five pcDNA vectors expressing POLA through POLD both i.d. and i.m. and one dose of a mixture of 2×10^7 PFU (each) of rVV-POLA, -POLB1, -POLB2, -POLC, and -POLD at 6-week intervals.

[b] DPI, day of euthanasia post-FIPV inoculation.

[c] WL, weight loss; F, fever; L, lymphopenia; J, jaundice as determined by plasma color.

[d] Th, thorax; Pe, peritoneum.

[e] Lu, lungs; P, pleura; Li, liver; K, kidney; S, spleen; I, intestine. (), minor lesions.

[f] NA, not applicable; ND, not determined.

[g] See also reference 16a.

critically determines disease progression and the ultimate outcome of the infection.

MATERIALS AND METHODS

Cells and viruses. Cells were maintained in Dulbecco's modified Eagle's medium (Life Technologies) supplemented with 10% fetal calf serum (Wisent), 100 IU of penicillin, and 100 μg of streptomycin per ml. FIPV serotype II strain 79–1146 (25) was propagated in *fcwf-D* cells and wild-type vaccinia virus (VV) strain WR and recombinant derivatives in RK13 cells, Ost7-1 cells, and human TK$^-$143 cells.

Animal experimentation. Specific pathogen-free (SPF) cats (Harlan Netherlands) were housed at the Central Animal Facility, Utrecht University. Experiments were performed in accordance with institutional and governmental guidelines after approval of the Animal Experimentation Ethics Committee of the Faculty of Veterinary Medicine. Thirty-three SPF cats, aged 5 to 7 months, which had been included in prime-boost vaccination trials with DNA vectors and recombinant VVs (rVVs), were inoculated with 500 to 1,000 PFU of FIPV strain 79–1146 6 weeks after the last boost. Details with respect to the vaccination history of each individual cat are listed in Table 1. The animals were monitored daily for body weight, rectal temperature, and gross clinical signs. EDTA-treated blood samples were taken two to three times per week to test for viremia by reverse transcription-PCR (RT-PCR). Plasma samples were prepared weekly to determine virus-neutralizing antibody titers. EDTA-treated and heparinized blood samples were collected weekly for leukocyte counting and CD4$^+$/CD8$^+$ staining, respectively.

Analysis of FIPV-neutralizing antibody titers. Neutralizing antibody titers were determined by end-point dilution as previously described (7). Briefly, 50 μl containing 100 PFU of FIPV strain 79–1146 was mixed with an equal volume of serial twofold dilutions of heat-inactivated plasma and preincubated at room temperature for 1 h. The virus-antibody mixtures were added to monolayers of *fcwf-D* cells, which had been seeded into microtiter plates 16 h in advance. All dilutions were tested in triplicate. The cytopathic effect was scored at 48 h after inoculation. Antibody titers were estimated according to Reed and Münch (37).

Histochemical and real-time RT-PCR analysis of blood samples. Whole-blood differentiation and leukocyte counting were performed by analysis of EDTA-treated blood by employing an ADVIA 120 Hematology System (Bayer Diagnostics). Immunophenotyping of heparinized blood samples was carried out by using fluorochrome-conjugated antisera: phycoerythrin-conjugated anti-feline CD4 and biotinylated anti-feline CD8 (Southern Biotechnology Associates, Inc.) in combination with Alexa-633-conjugated streptavidin (Molecular Probes). Per sample, 100,000 leukocytes were analyzed with a FACScalibur flow cytometer

TABLE 2. List of FIPV sequences expressed by recVVs

Insert name	Gene	Nct[a]	Nct[b]
POLA	*orf1a*	296–5198	−14 to 4889
POLB1	*orf1a*	5194–9447	4885–9138
POLB2	*orf1a*	9442–11990	9133–11681
POLC	*orf1b*	12684–16011	12375–15702[d]
POLD	*orf1b*	15914–20259	15605–19950[d]
3E7a	*3a*	24860–25075	1–216
3E7a	*3b*	25020–25235	1–216
3E7a	*3c*	25232–25966[c]	1–735
3E7a	*E*	25953–26201	1–249
3E7a	*7a*	28151–28456	1–306
7b	*7b*	28461–29081	1–621
S_I	*S*	20435–21913	1–1479
S_{II}	*S*	21164–22663	730–2229
S_{III}	*S*	21854–23365	1420–2931
S_{IV}	*S*	23306–24789	2872–4355

[a] Relative to the first nucleotide of the FIPV 79–1146 sequence (GenBank accession number).
[b] Relative to the first nucleotide of the ORF.
[c] The TAG stop codon in 3c at position 25352 was mutated into CAG, as is the case in canine coronavirus strain Insave.
[d] Relative to the first nucleotide of *orf1a*.

(Becton Dickinson) and the Windows-based WinMDI software (J. Trotter; http://facs.scripps.edu/software.html). Lymphocytes were selected in the forward and side scatter plots and gated for phycoerythrin-stained $CD4^+$ and AF633-stained $CD8^+$ T cells in the side scatter plots. Absolute T-cell counts per milliliter of whole blood were calculated from the frequencies of $CD4^+$ and $CD8^+$ T cells as determined by flow cytometry and the total leukocyte counts ([T cells/100,000] × [total leukocytes/ml]).

RNA was extracted from plasma and white blood cell pellets by using the QIAGEN viral RNA kit, and the equivalent of 8 μl of whole blood was subjected to FIPV-specific real-time RT-PCR essentially as previously described (15) in an ABI Prism 7000 Sequence Detection system (Applied Biosystems).

Construction of rVVs. rVVs expressing the FIPV S, M, and N proteins were described elsewhere (47, 48). Eleven additional rVVs were generated to express the 7b protein (rVV-7b), subfragments of pp1ab replicase polyprotein (rVV-POLA, rVV-POLB1, rVV-POLB2, rVV-POLC, and rVV-POLD), a chimeric gene comprising open reading frames (ORFs) 3a to 3c, the E gene, and ORF7a (rVV-3E7a), or overlapping subfragments of the S protein (rVV-S_I through -S_{IV}) (Table 2). With the exception of the 7b gene, genes and gene fragments were provided with an initiation codon and a 5′-terminal ubiquitin-encoding sequence. To ensure optimal expression of the pp1ab subfragments, cryptic VV transcription termination signals (TTTTNT) (13) were abolished. Proteolytic processing of pp1a expression products was prevented by rendering papain-like cystein proteinase 1 inactive through a C^{1117}→N substitution, and by devising the overall cloning strategy such that the coding sequences for papain-like cystein proteinase 2 and the chymotrypsin-like main proteinase were cleaved in two. The FIPV genes were cloned into transfer vector pSC11, downstream of the VV p7.5 early-late promoter, and rVVs were constructed as previously described (6). In all cases, expression of the FIPV genes was confirmed by radio immunoprecipitation assay with protein-specific antisera (data not shown).

Lymphocyte stimulation, cytokine staining, and flow cytometry. Single-cell spleen suspensions, prepared as previously described (10), were resuspended in 25 mM HEPES-buffered RPMI 1640 (Invitrogen Corporation), supplemented with 10% heat-inactivated fetal calf serum, Glutamax I (Invitrogen Corporation), 50 μM 2-mercaptoethanol, 100 IU of penicillin/ml, and 100 μg of streptomycin/ml. To detect FIPV-specific T cells, 0.5×10^6 to 1×10^6 splenocytes were stimulated for 6 h in the presence of 10 μM brefeldin A with autologous immortalized fibroblasts (5×10^4) (10), which had been infected with rVV for 16 h. Three-color flow cytometry analysis of virus-specific $CD4^+$ and $CD8^+$ T cells, based upon detection of intracellular tumor necrosis factor alpha (TNF-α), was performed as previously described (10).

RESULTS

Outline of longitudinal infection experiments. Thirty-three SPF cats were included in prime-boost vaccination trials employing DNA vectors and rVVs expressing nonstructural proteins of FIPV. Animals were challenged oronasally with 500 to 1,000 PFU of the highly virulent FIPV serotype II strain 79–1146 and monitored for up to 126 days postinfection (p.i.). Vaccination did not protect against or alter the course of the infection, as vaccinated and sham-vaccinated cats were similar with regard to the development of clinical signs and survival rate. Unfortunate though this may be, these extensive longitudinal experiments did provide a unique opportunity to study CoV-mediated disease progression in close detail.

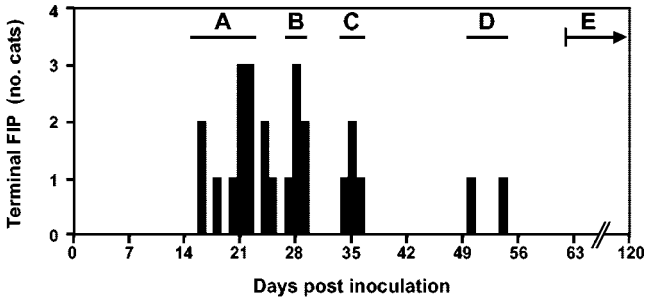

FIG. 1. Survival time and mortality after experimental FIPV infection. Bars indicate the number of animals succumbing to FIP per day. The labels A through E indicate groups of cats with distinct patterns of disease progression (see text).

Two animals (numbers 085 and 155) were sacrificed midinfection (see below); the remaining animals were followed throughout the complete course of the disease. Only six of these (19%) apparently made full recovery, surviving for more than 100 days. Twenty-five cats (81%) were euthanized in extremis with typical signs of FIP, 23 of these succumbing within 36 days p.i. (Fig. 1). In all cases, FIP diagnosis was confirmed upon postmortem examination, revealing pyogranulomatous lesions in major organs and intestines, peritoneal and/or pleural effusions, and a profound T-cell depletion. Survivors were free of lesions. All animals seroconverted. No differences were observed between survivors and FIP cases with respect to the onset of production and the final titers of neutralizing antibodies (Fig. 2). For detailed clinicopathological findings and vaccination status of the cats, see Table 1.

Disease progression in FIPV-infected cats. Disease progression was monitored by measuring body weight, rectal temperature, leukocyte counts, and the presence of viral RNA in plasma and white blood cells (Fig. 3). Irrespective of the final outcome, i.e., full-blown FIP or recovery, clinical signs were remarkably similar in all animals during the initial 7 to 8 days of infection and occurred with surprising synchronicity. A transient fever (>39.6°C) developed between days 2 to 4 p.i., lasting from 1 to 8 days (mean, 3.6 ± 1.7 days), which was invariably accompanied by progressive loss of body weight and acute lymphopenia ($\leq 1.5 \times 10^3$ lymphocytes/μl of blood). At day 8 p.i., body weight was reduced on average by 10% ± 2.6%, and lymphocyte numbers had dropped well below 50% of the initial counts (mean, 23.4% ± 16%; $0.7 \times 10^3 \pm 0.6 \times 10^3$ lymphocytes/μl). At 7 to 8 days p.i., disease progression seemingly halted: fever subsided, body weight either stabilized or increased, and the total number of peripheral blood lymphocytes started to rise again. This recovery, however, was only temporary; with the exception of survivor 289 (not shown), all

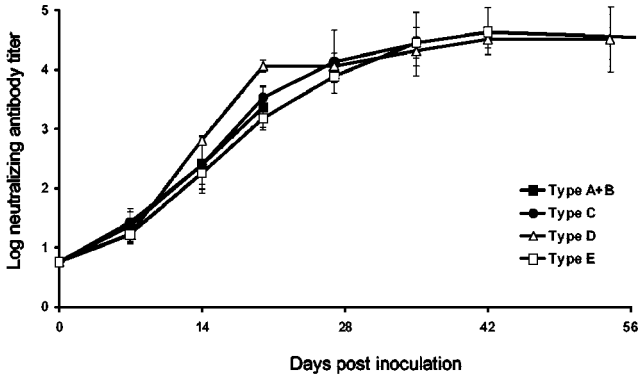

FIG. 2. Kinetics of neutralizing antibody titers in FIPV-infected cats with different types of disease progression. The virus-neutralizing antibody titers were determined weekly and are expressed as the reciprocal $\log_{10}$ plasma dilution causing 50% virus neutralization. The average titers of the rapid and intermediate (■, types A and B; 10 cats) and the delayed (●, type C; 3 cats) progressors and the prolonged (▲, type D; 2 cats) and long-term (□, type E, 5 cats) survivors are plotted on the *y* axis. Curves for types A and B were virtually identical and were therefore combined.

animals suffered a relapse. Starting from day 10, a second episode of fever developed. From this point on, five patterns of disease progression could be distinguished, based upon body weight and survival time (Fig. 1 and 3). Rapid progressors (type A) showed little to no regain in body weight during days 8 to 14 p.i., then developed a chronic secondary fever with severe wasting, and succumbed to FIP within 24 days (mean survival time, 21 ± 3 days). Intermediate and delayed progressors (types B and C) closely resembled type A but managed to regain body weight to almost 100% after the initial bout of disease and displayed increased survival times (mean, 28 ± 1 days and 35 ± 1 days, respectively). Prolonged survivors (cats 175 and 317; type D) developed an even more protracted course of the infection (survival times, 50 and 54 days, respectively) with three episodes of fever and weight loss and periods of up to 12 days of apparent recovery. Long-term survivors (type E) apparently succeeded in controlling the virus, in one case (cat 289) after the first wave of disease. The other animals suffered one or two relapses before ultimately gaining control.

Waves of FIPV replication coincide with fever, weight loss, and T-cell depletion. Previous experiments by our laboratory revealed that cats with terminal FIP are depleted for T cells both in the peripheral blood and in lymphoid tissues (16). In fact, we have now observed that the levels of peripheral $CD4^+$ and $CD8^+$ T lymphocytes dropped significantly very early in infection and, in those animals which developed fatal disease, remained low throughout the course of the infection (Fig. 3). During the short intermittent periods of apparent recovery, T-cell counts rose only to decline again with the renewed onset of disease. Episodes of disease coincided with an increase of viral RNA in plasma and/or white blood cells as measured by real-time and conventional RT-PCR (Fig. 3 and data not shown). Although FIPV primarily replicates in tissues, the amounts of viral RNA detected in the blood do provide a reflection—albeit most likely an underestimation—of the viral load at extravascular sites. Our combined data indicate that fever, wasting, and T-cell depletion all correlate with enhanced viral replication.

Virus-specific $CD8^+$ T-cell responses in FIPV survivors are mainly directed against S. Consistent with a prominent role of CMI in controlling FIPV infection and viral clearance, stimulation of splenocytes from FIP survivors with autologous FIPV-infected cells revealed virus-specific Th1-type T-cell responses, as measured by flow cytometric detection of intracellular TNF-α (10). To identify the relevant antigens, we constructed a library of 14 rVVs, which together express almost the entire FIPV 79–1146 proteome (Fig. 4; Table 2). Autologous fibroblast cultures were infected with these recombinant viruses and were used to stimulate splenocytes in our intracellular cytokine (TNF-α) staining assay (10). We analyzed T-cell responses in the spleen because it is both the major lymphoid organ harboring memory T cells and a prime target site for FIPV replication.

In addition to three long-term survivors (cats 249, 281, and 291), we studied two animals, numbers 155 and 085, which were sacrificed midinfection at day 42 and 58 p.i., respectively. One of these, number 155, displayed only mild clinical signs; after a short relapse, it quickly recovered and remained seemingly healthy. The other experienced chronic fever and stayed underweight from day 21 p.i. onward. Although both animals were persistently infected, as evidenced by RT-PCR detection of viral RNA in the blood (Fig. 3F), no FIP lesions were found upon postmortem analysis. Apparently, these cats had acquired at least partial immunity in response to FIPV infection.

In all five cats, the S protein was identified as the main $CD8^+$ T-cell antigen (Fig. 5 and 6). The S protein apparently contains multiple $CD8^+$ T-cell epitopes, as shown by lymphocyte stimulation assays with rVVs expressing overlapping S subfragments (Fig. 4; Table 3). In cat 155, responses were exclusively directed against S_I, indicating that a $CD8^+$ T-cell epitope was located within the N-terminal-most 250 residues of S. Cat 249 recognized both S_{II} and S_{III}, suggesting the presence of an epitope in the 270-residue overlapping region (residues 474 to 743). Finally, cat 291 presumably harbored $CD8^+$ memory T cells directed against two epitopes, one in the C-terminal half of subfragment S_{III} (residues 744 to 977), the other in S_{IV} (residues 958 to 1452; S_{III} and S_{IV} share only a 20-amino-acid overlap). In long-term survivors 281 and 291, $CD8^+$ T-cell responses seemed exclusively directed against the S protein. In long-term survivor 249 and in the partially protected animals 085 and 155, subdominant $CD8^+$ T-cell responses were detected against the pp1a B2 subfragment (085), the M protein (cats 085 and 249), and the chimeric protein 3E7a (cats 155 and 249). The S protein also seemed to be a prominent target for antiviral $CD4^+$ T cells, although considerable responses against other antigens, most notably M, were also detected (Fig. 5 and 6).

DISCUSSION

FIP, a paradigm of CoV-mediated chronic disease, was already recognized in earlier studies as a complex multiphasic condition with recurrent (biphasic) fever as one of its most distinctive traits (41, 47, 50, 53). The pathogenic mechanisms, however, remain poorly understood. Here, we extend previous findings (16, 32, 50, 53) and present a comprehensive study of

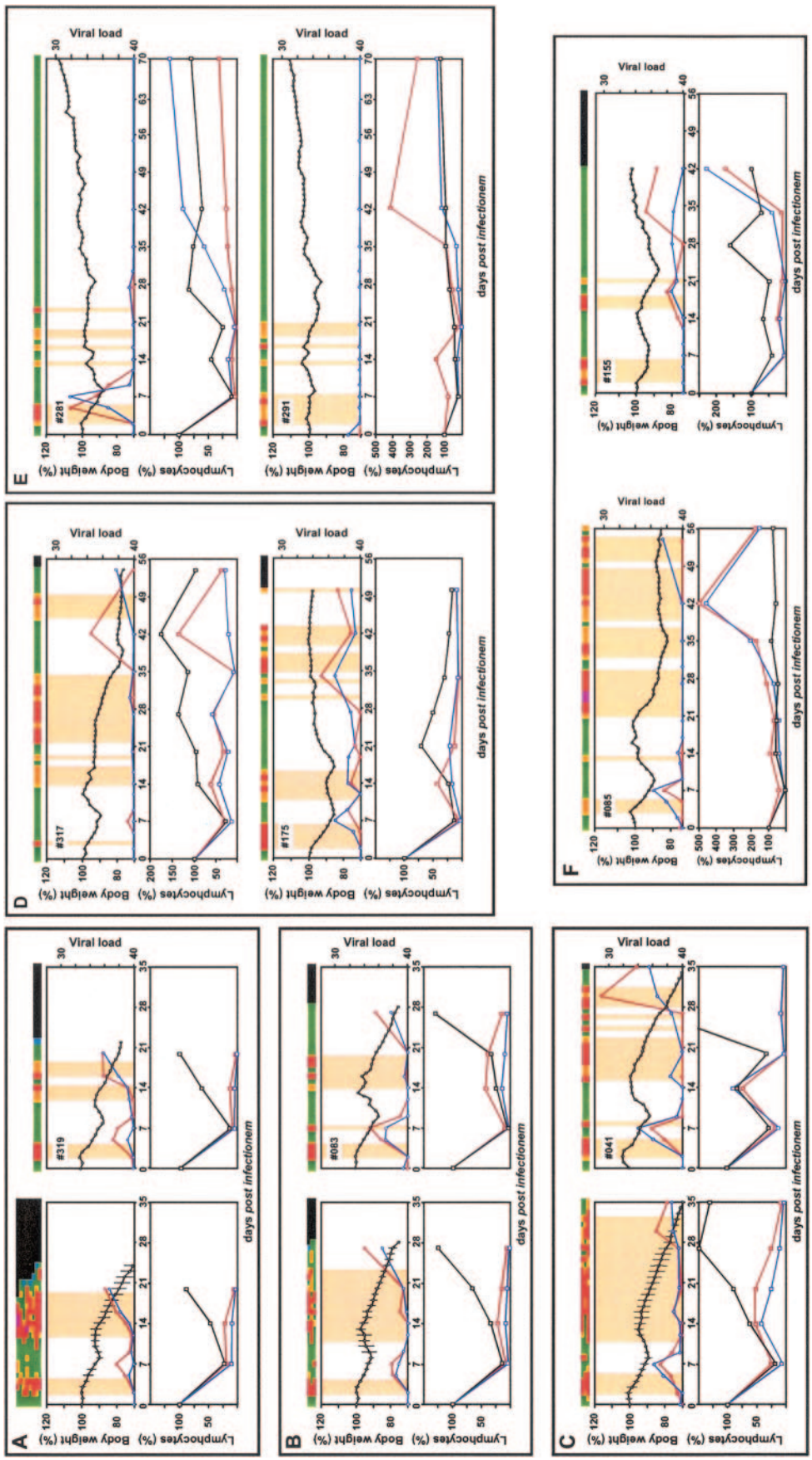

FIG. 3. Disease progression in rapid (A), intermediate (B), and delayed (C) progressors and in prolonged (D) and long-term (E) FIPV survivors. Cats, inoculated oronasally with FIPV 79–1146, were monitored for up to 126 days for fever, body weight, and viral RNA in white blood cells and plasma (top graphs). In addition, total lymphocyte counts and $CD4^+$ and $CD8^+$ T-cells counts (black, red and blue lines, respectively) were determined (bottom graphs). Periods of fever are indicated by pink shading and color coding as follows: blue, ≤37°C; green, 37 to 39.7°C; orange, 39.7 to 40°C; red, 40 to 41°C; magenta, ≥41°C. Body weight (black line, open circles) is expressed as the percentage of weight at day 0. Viral RNA titers as determined by real-time RT-PCR are expressed as C_T values on an inverted *y* axis (red line, white blood cells; blue line, plasma). Total lymphocyte and T-cell counts are presented as percentages of the cell counts determined at day 0. For groups A to C, data acquired for animals with highly similar disease progression were averaged ($n = 7$, 3, and 3 cats, respectively) to obtain trend curves (left-hand panels). Results obtained for individual animals are shown on the right. For groups D and E, only data for individual animals are presented; for group E, two representative examples are shown. (F) Disease progression in persistently infected cats 085 and 155. The animals were sacrificed at days 58 and 42, respectively.

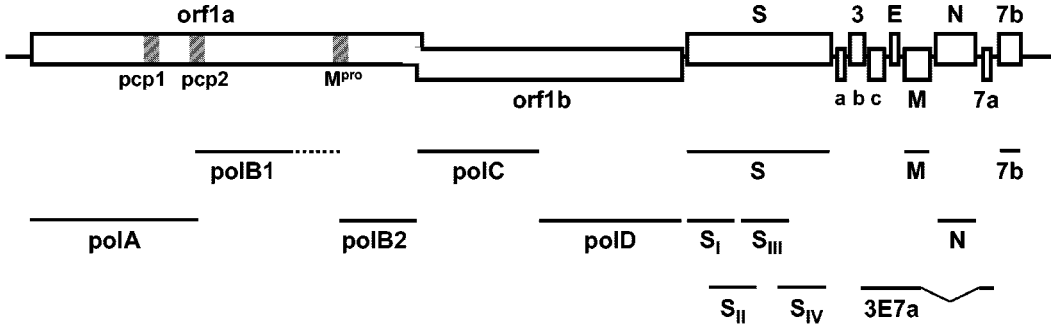

FIG. 4. rVV expression library of the FIPV 79–1146 proteome. The viral genome is shown schematically. Depicted as boxes are the coding sequences for polyprotein pp1ab (ORF1a and ORF1b), the spike protein (S), the small membrane protein (E), the membrane protein (M), the nucleocapsid protein (N), and those for the accessory proteins 3a to 3c, 7a, and 7b. Indicated below are the regions expressed by the various rVVs (Table 2).

the natural history, viral dynamics, and immunobiology of FIP. In a longitudinal experiment, we followed disease progression in a large cohort of cats after oronasal infection with the highly virulent FIPV strain 79–1146. We found that the very early stages of experimentally induced FIP were virtually identical among the different animals, irrespective of the final outcome, i.e., death or recovery. All cats presented characteristic signs of acute infection with fever, weight loss, acute lymphopenia, and the presence of viral RNA in blood cells and plasma. Then, by day 7 to 8 p.i., disease seemingly resolved and the animals improved: fever subsided, body weight stabilized or increased, and the amounts of viral RNA in the blood decreased below detection levels. However, all cats but one suffered a major relapse, and most of them inexorably progressed to lethal dis-

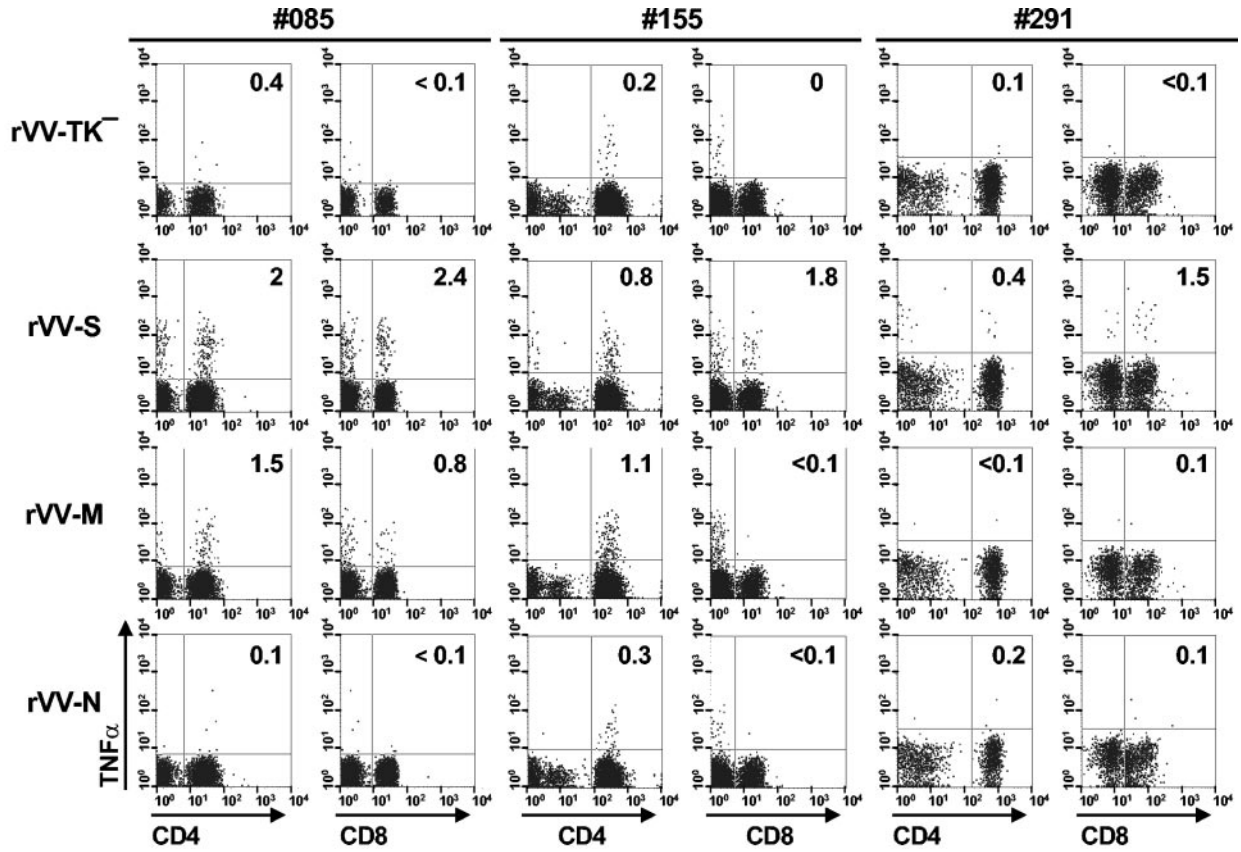

FIG. 5. FIPV-specific T-cell responses in persistently infected, partially protected cats and in a long-term survivor. Splenocytes were stimulated with autologous fibroblast cultures (10), which had been infected with rVVs expressing the various FIPV proteins. An rVV with *lacZ* inserted into the TK locus (rVV-TK) served as a negative control. Only the results obtained with rVV-TK, rVV-S, rVV-M, and rVV-N are shown. Virus-specific $CD4^+$ and $CD8^+$ T cells were identified by intracellular expression of TNF-α by three-color flow cytometry. Results obtained for partially protected animals 085 and 155 and for long-term survivor 291 are shown as dot-plot representations, with frequencies of antigen-specific T cells given as percentages of the total $CD4^+$ or $CD8^+$ populations.

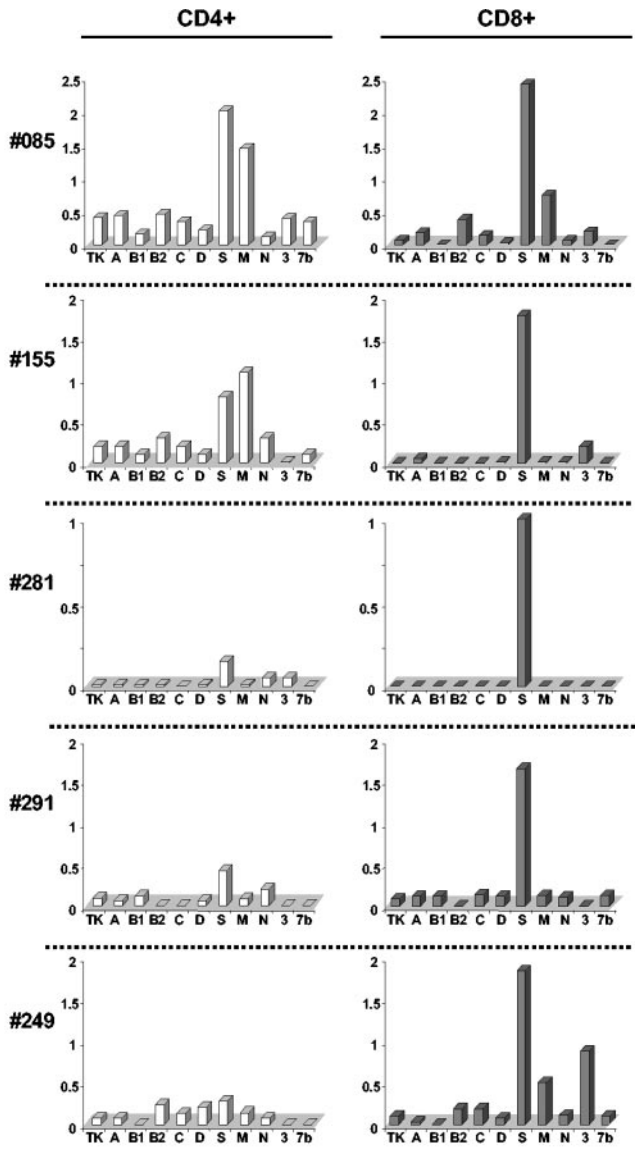

FIG. 6. FIPV-specific T-cell responses in persistently infected, partially protected cats and in long-term survivors. Splenocytes were stimulated with autologous fibroblast cultures (10), which had been mock infected or infected with rVVs expressing FIPV proteins (A through 7b; 3 indicates 3E7a) (see Fig. 4). rVV-TK served as a negative control (TK). Virus-specific T cells were identified by intracellular expression of TNF-α by three-color flow cytometry. The results are presented as bar graphs, depicting the antigen-specific $CD4^+$ and $CD8^+$ T-cell responses in persistently infected animals (cats 085 and 155) and in long-term survivors (cats 249, 281, and 291). Frequencies of antigen-specific T cells (*y* axis) are given as percentages of the total $CD4^+$ or $CD8^+$ populations.

ease within 16 to 54 days. We distinguished five groups on the basis of survival time, which were operationlly designated as rapid, intermediate, or delayed progressors and prolonged or long-term survivors. Animals in the latter two groups succeeded in countering the second wave of disease either to succumb to a subsequent, final relapse or to gain apparent control of the infection, respectively. It is unknown whether long-term survivors really achieved complete viral clearance or

TABLE 3. $CD8^+$ T-cell responses against S subfragments[a]

	TK^-	S_I	S_{II}	S_{III}	S_{IV}
155	0	**1.8**	0.1	0.2	<0.1
249	<0.1	0.1	**0.6**	**0.4**	<0.1
291	0	0.1	0.1	**0.4**	**0.7**

[a] Frequencies of TNF-α-producing $CD8^+$ T cells are given as percentages of the total CD8+ T-cell population. Data in boldface type represent the frequencies of S protein-specific T cells.

remained persistently infected at a low level. In similar cases, FIP could be induced even up to 1 year after initial FIPV inoculation by performing a superinfection with the immunosuppressive feline leukemia virus (33).

Perhaps the most intriguing aspect of FIPV infection is its effect on the $CD4^+$ and $CD8^+$ T-cell levels. FIPV-induced T-cell depletion has been documented before (16, 21), but we are first to show that this phenomenon already occurs very early in infection and correlates with (enhanced) viral replication. After the initial general lymphopenia, total lymphocyte numbers rose again and remained at levels equal to or exceeding those at day 0. In contrast, $CD4^+$ and $CD8^+$ T-cell counts remained consistently low. During the periods of apparent convalescence, T-cell counts increased modestly only to fall again with the renewed onset of overt disease. In agreement with earlier reports (16, 21), T cells were virtually depleted from lymphatic tissue and from peripheral tissue in the animals with end-stage FIP. How FIPV causes T-cell lymphopenia is not clear. As there are no indications that T cells are susceptible to infection, their depletion most likely occurs through indirect effects (16). In other examples of virus-induced T-cell depletion, e.g., measles, the infection of antigen-presenting cells, and of dendritic cells (DCs) in particular, is thought to cause T-cell apoptosis (28, 30, 38, 39). Likewise, FIPV reportedly targets antigen-presenting cells, such as macrophages and monocytes (16, 29, 40, 52), the serotype II strains via the dedicated cell receptor CD13 (43). Given the fact that human immature myeloid DCs express CD13 (42), it is likely that certain DC subsets of the cat do so as well and hence are susceptible to FIPV.

We propose that the virus-driven T-cell depletion results in an acute immunodeficiency and that in the early stages of infection the immune system is already facing an uphill struggle. Still, all animals were able to at least temporarily contain the first wave of disease. In agreement with the general view that humoral immunity is not protective, virus-neutralizing antibodies appeared and rose with identical kinetics and to similar titers in survivors and nonsurvivors (Fig. 2). Moreover, antibodies seem to be generated too late during the course of acute FIPV infection to contribute to host defenses. We therefore assume that the partial control of viral replication, which occurs during the early days after infection, is primarily T-cell mediated. Indeed, the onset of apparent convalescence around day 7 p.i. would correlate temporally with the expected peak of the early virus-specific effector $CD8^+$ T-cell response, as described with other systems (1, 26).

Our combined observations are therefore consistent with a model for FIP pathogenesis in which virus-induced T-cell depletion and the antiviral T-cell responses are opposing forces.

The net result is an intermittent infection, with episodes of disease driven by enhanced viral replication punctuated by short periods of apparent convalescence. The efficacy of the primary T-cell responses most likely determines to what extent the initial wave of infection can be contained and hence would be the decisive factor in disease progression. If the first response is too weak, a second wave of increased virus replication will further reduce T-cell numbers and swiftly overwhelm the immune system (rapid progressors; type A) (Fig. 3). If, however, the initial T-cell responses succeed in largely containing viral replication, the animal may develop a more protracted course of the disease (delayed progressors; type C) (Fig. 3) or even get a second chance (prolonged and long-term survivors; types D and E) (Fig. 3). The rising amounts of viral RNA in the blood, consistently seen in animals with end-stage FIP, indicate that progression to fatal disease is the direct consequence of a loss of immune control, ultimately resulting in unchecked viral replication. Whether or not an animal is able to mount a protective immune response may be determined at least in part by its haplotype. Indeed, cheetahs (*Acinonyx jubatus*) are extremely sensitive to FIP, a peculiarity which has been ascribed to their genetic uniformity and their lack of major histocompatibility complex class I polymorphism (27).

If CMI does confer protection, the question arises as to which viral antigens are involved. Our analysis of the specificity of splenic (memory) T-cell pools in three long-term survivors and in two persistently infected, partially protected animals identified the spike protein as the dominant target for $CD8^+$ T cells. The immunodominance of epitopes from a viral envelope glycoprotein after chronic infection is reminiscent of the situation in inbred mice chronically infected with the mouse hepatitis CoV (MHV) or with the lymphocytic choriomeningitis arenavirus (LCMV). In both cases, immunodominance shifted during the course of persistent infection from epitopes on the highly expressed cytoplasmic nucleocapsid proteins (N for MHV and NP for LCMV) towards those from the envelope glycoproteins (S for MHV and GP for LCMV) (3, 46, 55). In LCMV-infected animals, the NP-specific $CD8^+$ T cells undergo rapid inactivation (exhaustion) or even deletion as a result of antigenic overstimulation (55). A similar mechanism has been postulated to explain the inversion of immunodominance during chronic MHV infection (3). It is therefore tempting to speculate that the immunodominance of S-derived $CD8^+$ T-cell epitopes after chronic FIPV infection reflects the selective survival of S-specific $CD8^+$ T cells at the expense of T cells recognizing epitopes of other viral proteins, in particular of N (46). The apparent dominance of S-derived epitopes becomes even more remarkable if one takes into account that cats are outbred. Indeed, the anti-S responses measured in individual cats were directed against different epitopes, implying that the immunodominance of S did not merely reflect the chance dominance of a single epitope-major histocompatibility complex class I combination.

The pathogenic phenomena described here may not be limited to FIP but likely bear relevance to the immunobiology and pathogenesis of other chronic CoV infections, in particular of SARS, for which acute T-cell lymphopenia, multiphasic disease, and viral persistence have been previously reported (2, 4, 8, 12, 24, 36, 44, 56). FIP presents a relevant, safe, and well-defined model to study CoV-mediated immunosuppression. Moreover, as disease progression is highly reproducible and primarily driven by viral replication, it should provide an attractive and convenient model system for in vivo testing of anti-CoV drugs.

ACKNOWLEDGMENTS

We thank Rachida Siamari, Ben van Schaijk, and the personnel of the Infection Unit (Central Animal Facility, University of Utrecht) for excellent technical assistance; Herman Egberink for his help with the animal experiments; Fermin Simons and Liesbeth Breure-Vogel for advice concerning real-time RT-PCR; and Bert-Jan Haijema for sharing materials.

Our research was supported by a grant from Intervet International B.V.

REFERENCES

1. **Benlhassan-Chahour, K., C. Penit, V. Dioszeghy, F. Vasseur, G. Janvier, Y. Riviere, N. Dereuddre-Bosquet, D. Dormont, R. Le Grand, and B. Vaslin.** 2003. Kinetics of lymphocyte proliferation during primary immune response in macaques infected with pathogenic simian immunodeficiency virus SIVmac251: preliminary report of the effect of early antiviral therapy. J. Virol. **77:**12479–12493.
2. **Berger, A., C. Drosten, H. W. Doerr, M. Sturmer, and W. Preiser.** 2004. Severe acute respiratory syndrome (SARS)-paradigm of an emerging viral infection. J. Clin. Virol. **29:**13–22.
3. **Bergmann, C. C., J. D. Altman, D. Hinton, and S. A. Stohlman.** 1999. Inverted immunodominance and impaired cytolytic function of CD8+ T cells during viral persistence in the central nervous system. J. Immunol. **163:**3379–3387.
4. **Booth, C. M., L. M. Matukas, G. A. Tomlinson, A. R. Rachlis, D. B. Rose, H. A. Dwosh, S. L. Walmsley, T. Mazzulli, M. Avendano, P. Derkach, I. E. Ephtimios, I. Kitai, B. D. Mederski, S. B. Shadowitz, W. L. Gold, L. A. Hawryluck, E. Rea, J. S. Chenkin, D. W. Cescon, S. M. Poutanen, and A. S. Detsky.** 2003. Clinical features and short-term outcomes of 144 patients with SARS in the greater Toronto area. JAMA **289:**2801–2809.
5. **Brown, T. D. K., and I. Brierly.** 1995. The coronaviral nonstructural proteins, p. 191–217. *In* S. G. Siddell (ed.), The *Coronaviridae*. Plenum Press, New York, N.Y.
6. **Chakrabarti, S., K. Brechling, and B. Moss.** 1985. Vaccinia virus expression vector: coexpression of beta-galactosidase provides visual screening of recombinant virus plaques. Mol. Cell. Biol. **5:**3403–3409.
7. **Corapi, W. V., C. W. Olsen, and F. W. Scott.** 1992. Monoclonal antibody analysis of neutralization and antibody-dependent enhancement of feline infectious peritonitis virus. J. Virol. **66:**6695–6705.
8. **Cui, W., Y. Fan, W. Wu, F. Zhang, J. Y. Wang, and A. P. Ni.** 2003. Expression of lymphocytes and lymphocyte subsets in patients with severe acute respiratory syndrome. Clin. Infect. Dis. **37:**857–859.
9. **de Groot, R. J., and M. C. Horzinek.** 1995. Feline infectious peritonitis, p. 239–309. *In* S. G. Siddell (ed.), The *Coronaviridae*. Plenum Press, New York, N.Y.
10. **de Groot-Mijnes, J. D. F., R. G. van der Most, J. M. van Dun, E. G. te Lintelo, N. M. P. Schuurman, H. F. Egberink, and R. J. de Groot.** 2004. Three-color flow cytometry detection of virus-specific CD4+ and CD8+ T cells in the cat. J. Immunol. Methods **285:**41–54.
11. **de Vries, A. A. F., M. C. Horzinek, P. J. M. Rottier, and R. J. de Groot.** 1997. The genome organization of the nidovirales: similarities and differences between arteri-, toro-, and coronaviruses. Semin. Virol. **8:**33–47.
12. **Drosten, C., S. Gunther, W. Preiser, S. van der Werf, H. R. Brodt, S. Becker, H. Rabenau, M. Panning, L. Kolesnikova, R. A. Fouchier, A. Berger, A. M. Burguiere, J. Cinatl, M. Eickmann, N. Escriou, K. Grywna, S. Kramme, J. C. Manuguerra, S. Muller, V. Rickerts, M. Sturmer, S. Vieth, H. D. Klenk, A. D. Osterhaus, H. Schmitz, and H. W. Doerr.** 2003. Identification of a novel coronavirus in patients with severe acute respiratory syndrome. N. Engl. J. Med. **348:**1967–1976.
13. **Earl, P. L., A. W. Hugin, and B. Moss.** 1990. Removal of cryptic poxvirus transcription termination signals from the human immunodeficiency virus type 1 envelope gene enhances expression and immunogenicity of a recombinant vaccinia virus. J. Virol. **64:**2448–2451.
14. **Fouchier, R. A., N. G. Hartwig, T. M. Bestebroer, B. Niemeyer, J. C. De Jong, J. H. Simon, and A. D. Osterhaus.** 2004. A previously undescribed coronavirus associated with respiratory disease in humans. Proc. Natl. Acad. Sci. USA **101:**6212–6216.
15. **Gut, M., C. M. Leutenegger, J. B. Huder, N. C. Pedersen, and H. Lutz.** 1999. One-tube fluorogenic reverse transcription-polymerase chain reaction for the quantitation of feline coronaviruses. J. Virol. Methods **77:**37–46.
16. **Haagmans, B. L., H. F. Egberink, and M. C. Horzinek.** 1996. Apoptosis and T-cell depletion during feline infectious peritonitis. J. Virol. **70:**8977–8983.

16a. **Haijema, B. J., H. Volders, and P. J. M. Rottier.** 2004. Live, attenuated

coronavirus vaccines through the directed deletion of group-specific genes provide protection against feline infectious peritonitis. J. Virol. **78:**3863–3871.
17. **Hayashi, T., N. Sasaki, Y. Ami, and K. Fujiwara.** 1983. Role of thymus-dependent lymphocytes and antibodies in feline infectious peritonitis after oral infection. Nippon Juigaku Zasshi **45:**759–766.
18. **Herrewegh, A. A., H. Vennema, M. C. Horzinek, P. J. Rottier, and R. J. de Groot.** 1995. The molecular genetics of feline coronaviruses: comparative sequence analysis of the ORF7a/7b transcription unit of different biotypes. Virology **212:**622–631.
19. **Hohdatsu, T., M. Nakamura, Y. Ishizuka, H. Yamada, and H. Koyama.** 1991. A study on the mechanism of antibody-dependent enhancement of feline infectious peritonitis virus infection in feline macrophages by monoclonal antibodies. Arch. Virol. **120:**207–217.
20. **Hunziker, L., M. Recher, A. J. Macpherson, A. Ciurea, S. Freigang, H. Hengartner, and R. M. Zinkernagel.** 2003. Hypergammaglobulinemia and autoantibody induction mechanisms in viral infections. Nat. Immunol. **4:**343–349.
21. **Kipar, A., K. Kohler, W. Leukert, and M. Reinacher.** 2001. A comparison of lymphatic tissues from cats with spontaneous feline infectious peritonitis (FIP), cats with FIP virus infection but no FIP, and cats with no infection. J. Comp. Pathol. **125:**182–191.
22. **Ksiazek, T. G., D. Erdman, C. S. Goldsmith, S. R. Zaki, T. Peret, S. Emery, S. Tong, C. Urbani, J. A. Comer, W. Lim, P. E. Rollin, S. F. Dowell, A. E. Ling, C. D. Humphrey, W. J. Shieh, J. Guarner, C. D. Paddock, P. Rota, B. Fields, J. DeRisi, J. Y. Yang, N. Cox, J. M. Hughes, J. W. LeDuc, W. J. Bellini, and L. J. Anderson.** 2003. A novel coronavirus associated with severe acute respiratory syndrome. N. Engl. J. Med. **348:**1953–1966.
23. **Lee, N., D. Hui, A. Wu, P. Chan, P. Cameron, G. M. Joynt, A. Ahuja, M. Y. Yung, C. B. Leung, K. F. To, S. F. Lui, C. C. Szeto, S. Chung, and J. J. Sung.** 2003. A major outbreak of severe acute respiratory syndrome in Hong Kong. N. Engl. J. Med. **348:**1986–1994.
24. **Leung, W. K., K. To, P. K. S. Chan, H. L. Y. Chan, A. K. L. Wu, N. Lee, K. Y. Yuen, and J. J. Y. Sung.** 2003. Enteric involvement of severe acute respiratory syndrome-associated coronavirus infection. Gastroenterology **125:**1011–1017.
25. **McKeirnan, A. J., J. F. Evermann, A. Hargis, and R. L. Ott.** 1981. Isolation of feline coronaviruses from two cats with diverse disease manifestations. Feline Pract. **11:**17–20.
26. **Murali-Krishna, K., J. D. Altman, M. Suresh, D. J. Sourdive, A. J. Zajac, J. D. Miller, J. Slansky, and R. Ahmed.** 1998. Counting antigen-specific CD8 T cells: a reevaluation of bystander activation during viral infection. Immunity **8:**177–187.
27. **O'Brien, S. J., M. E. Roelke, L. Marker, A. Newman, C. A. Winkler, D. Meltzer, L. Colly, J. F. Evermann, M. Bush, and D. E. Wildt.** 1985. Genetic basis for species vulnerability in the cheetah. Science **227:**1428–1434.
28. **Okada, H., F. Kobune, T. A. Sato, T. Kohama, Y. Takeuchi, T. Abe, N. Takayama, T. Tsuchiya, and M. Tashiro.** 2000. Extensive lymphopenia due to apoptosis of uninfected lymphocytes in acute measles patients. Arch. Virol. **145:**905–920.
29. **Paltrinieri, S., M. P. Cammarata, G. Cammarata, and S. Comazzi.** 1998. Some aspects of humoral and cellular immunity in naturally occuring feline infectious peritonitis. Vet. Immunol. Immunopathol. **65:**205–220.
30. **Palucka, K., and J. Banchereau.** 2002. How dendritic cells and microbes interact to elicit or subvert protective immune responses. Curr. Opin. Immunol. **14:**420–431.
31. **Pedersen, N. C., and J. F. Boyle.** 1980. Immunological phenomena in the effusive form of feline infectious peritonitis. Am. J. Vet. Res. **41:**868–876.
32. **Pedersen, N. C., J. F. Evermann, A. J. McKeirnan, and R. L. Ott.** 1984. Pathogenicity studies of feline coronavirus isolates 79–1146 and 79–1683. Am. J. Vet. Res. **45:**2580–2585.
33. **Pedersen, N. C., and K. Floyd.** 1985. Experimental studies with three new strains of feline infectious peritonitis virus: FIPV-UCD2, FIPV-UCD3 and FIPV-UCD4. Compend. Contin. Educ. Pract. Vet. **7:**1001–1011.
34. **Peiris, J. S., S. T. Lai, L. L. Poon, Y. Guan, L. Y. Yam, W. Lim, J. Nicholls, W. K. Yee, W. W. Yan, M. T. Cheung, V. C. Cheng, K. H. Chan, D. N. Tsang, R. W. Yung, T. K. Ng, and K. Y. Yuen.** 2003. Coronavirus as a possible cause of severe acute respiratory syndrome. Lancet **361:**1319–1325.
35. **Poland, A. M., H. Vennema, J. E. Foley, and N. C. Pedersen.** 1996. Two related strains of feline infectious peritonitis virus isolated from immunocompromised cats infected with a feline enteric coronavirus. J. Clin. Microbiol. **34:**3180–3184.
36. **Poutanen, S. M., D. E. Low, B. Henry, S. Finkelstein, D. Rose, K. Green, R. Tellier, R. Draker, D. Adachi, M. Ayers, A. K. Chan, D. M. Skowronski, I. Salit, A. E. Simor, A. S. Slutsky, P. W. Doyle, M. Krajden, M. Petric, R. C. Brunham, and A. J. McGeer.** 2003. Identification of severe acute respiratory syndrome in Canada. N. Engl. J. Med. **348:**1995–2005.
37. **Reed, L. H., and H. Münch.** 1938. A simple method for estimating 50 percent endpoints. Am. J. Hyg. **27:**493–497.
38. **Schneider-Schaulies, S., K. Bieback, E. Avota, I. Klagge, and V. ter Meulen.** 2002. Regulation of gene expression in lymphocytes and antigen-presenting cells by measles virus: consequences for immunomodulation. J. Mol. Med. **80:**73–85.
39. **Servet-Delprat, C., P. O. Vidalain, H. Valentin, and C. Rabourdin-Combe.** 2003. Measles virus and dendritic cell functions: how specific response cohabits with immunosuppression. Curr. Top. Microbiol. Immunol. **276:**103–123.
40. **Stoddart, C. A., and F. W. Scott.** 1988. Isolation and identification of feline peritoneal macrophages for in vitro studies of coronavirus-macrophage interactions. J. Leukoc. Biol. **44:**319–328.
41. **Stoddart, M. E., J. T. Whicher, and D. A. Harbour.** 1988. Cats inoculated with feline infectious peritonitis virus exhibit a biphasic acute phase plasma protein response. Vet. Rec. **123:**622–624.
42. **Summers, K. L., B. D. Hock, J. L. McKenzie, and D. N. Hart.** 2001. Phenotypic characterization of five dendritic cell subsets in human tonsils. Am. J. Pathol. **159:**285–295.
43. **Tresnan, D. B., R. Levis, and K. V. Holmes.** 1996. Feline aminopeptidase N serves as a receptor for feline, canine, porcine, and human coronaviruses in serogroup I. J. Virol. **70:**8669–8674.
44. **Tsang, O. T., T. N. Chau, K. W. Choi, E. Y. K. Tso, W. Lim, M. C. Chiu, W. L. Tong, P. O. Lee, B. H. S. Lam, T. K. Ng, J. Y. Lai, W. C. Yu, and S. T. Lai.** 2003. Severe acute respiratory syndrome: recurrence? Hospital infection? Emerg. Infect. Dis. **9:**1180–1181.
45. **van der Hoek, L., K. Pyrc, M. F. Jebbink, W. Vermeulen-Oost, R. J. M. Berkhout, K. C. Wolthers, P. M. E. Wertheim-van Dillen, J. Kaandorp, J. Spaargaren, and B. Berkhout.** 2004. Indentification of a new human coronavirus. Nat. Med. **10:**368–373.
46. **van der Most, R. G., K. Murali-Krishna, J. G. Lanier, E. J. Wherry, M. T. Puglielli, J. N. Blattman, A. Sette, and R. Ahmed.** 2003. Changing immunodominance patterns in antiviral CD8 T-cell responses after loss of epitope presentation or chronic antigenic stimulation. Virology **315:**93–102.
47. **Vennema, H., R. J. de Groot, D. A. Harbour, M. Dalderup, T. Gruffydd-Jones, M. C. Horzinek, and W. J. Spaan.** 1990. Early death after feline infectious peritonitis virus challenge due to recombinant vaccinia virus immunization. J. Virol. **64:**1407–1409.
48. **Vennema, H., R. J. de Groot, D. A. Harbour, M. C. Horzinek, and W. J. Spaan.** 1991. Primary structure of the membrane and nucleocapsid protein genes of feline infectious peritonitis virus and immunogenicity of recombinant vaccinia viruses in kittens. Virology **181:**327–335.
49. **Vennema, H., A. Poland, J. Foley, and N. C. Pedersen.** 1998. Feline infectious peritonitis viruses arise by mutation from endemic feline enteric coronaviruses. Virology **243:**150–157.
50. **Ward, J. M., D. H. Gribble, and D. L. Dungworth.** 1974. Feline infectious peritonitis: experimental evidence for its multiphasic nature. Am. J. Vet. Res. **35:**1271–1275.
51. **Weiss, R. C., and N. R. Cox.** 1989. Evaluation of immunity to feline infectious peritonitis in cats with cutaneous viral-induced delayed hypersensitivity. Vet. Immunol. Immunopathol. **21:**293–309.
52. **Weiss, R. C., and F. W. Scott.** 1981. Antibody-mediated enhancement of disease in feline infectious peritonitis: comparisons with dengue hemorrhagic fever. Comp. Immunol. Microbiol. Infect. Dis. **4:**175–189.
53. **Weiss, R. C., and F. W. Scott.** 1981. Pathogenesis of feline infectious peritonitis: nature and development of viremia. Am. J. Vet. Res. **42:**382–390.
54. **Weiss, R. C., and F. W. Scott.** 1981. Pathogenesis of feline infectious peritonitis: pathologic changes and immunofluorescence. Am. J. Vet. Res. **42:**2036–2048.
55. **Wherry, E. J., J. N. Blattman, K. Murali-Krishna, R. van der Most, and R. Ahmed.** 2003. Viral persistence alters CD8 T-cell immunodominance and tissue distribution and results in distinct stages of functional impairment. J. Virol. **77:**4911–4927.
56. **Wong, R. S., A. Wu, K. F. To, N. Lee, C. W. Lam, C. K. Wong, P. K. Chan, M. H. Ng, L. M. Yu, D. S. Hui, J. S. Tam, G. Cheng, and J. J. Sung.** 2003. Haematological manifestations in patients with severe acute respiratory syndrome: retrospective analysis. BMJ **326:**1358–1362.